THE DISTRIBUTION OF PRESSURE OVER THE SURFACE OF AIRSHIP MODEL U.721, TOGETHER WITH A COMPARISON WITH THE PRESSURE OVER A SPHEROID.

By R. JONES, M.A., and D. H. WILLIAMS, B.Sc.

Reports and Memoranda, No. 600. *April,* 1919.

SUMMARY.—(*a*) *Introductory : Reasons for Inquiry.*—Investigation undertaken at the request of Airship Design Department of the Admiralty to obtain data upon which to base nose-stiffening calculations on new airship.

(*b*) *Range of Investigation.*—Distribution of pressure was measured over the whole length of the airship model at zero angle of incidence, with wind speed varying from 30 to 75 ft/sec. Also the pressures were measured on the nose of the model at different angles of yaw ($-20°$ to $+20°$) and roll ($-90°$ to $+90°$), at a wind speed of 40 ft/sec. A cone tangential to the model at a point near the nose was added, and the pressures aft of the circle of contact measured.

Pressures also measured on a spheroid ratio of axes, 4 : 1, similar to head of airship model, at speeds of 40 and 60 ft/sec., and angles of incidence $-10°$, $0°$ and $+10°$.

Theoretical investigation of pressures over the spheroid is included for a wide range of angle of yaw and roll.

(*c*) *Conclusions.*—The pressure aft of circle of contact of tangent cone at the nose does not appear to be affected by the cone.

Agreement between the theoretical and experimental pressures on spheroid good, and if a spheroid be found that fits the airship model near the nose the theoretical pressures on this spheroid agree with the experimental pressures on the airship, provided the $\frac{1}{2}\rho V^2$ point on the former be taken at the nose of the latter.

General nature of variation with angle of roll similar for the spheroid airship model head.

Integration of pressures over the surface of airship model at zero incidence gives a negative value for form resistance. This is more marked on account of the correction applied for variation of static pressure down the channel.

(*d*) *Applications and further developments.*—It is suggested that the pressure variation over the nose of a model, whose shape in that region is approximately a spheroid, can be calculated theoretically—at least as far as the point where the pressure is one-tenth of ρV^2—and that is the part that has to be considered in connection with nose stiffening investigations. It is well to note that an airship form, in which the high pressures are concentrated over a small area, can be more easily constructed with a satisfactory margin of strength than one in which the pressure is more evenly distributed.

Further, in view of the uncertainty of the correction to be applied to the form resistance to allow for static pressure variation (it is of the same order of magnitude as the form resistance), it would appear that experiments should be conducted with a view to eliminating the correction altogether.

The experiments described in the present report were undertaken at the request of the Airship Design Department of the Admiralty, with a view to obtaining information that would be of value in connection with stiffening the nose of a new type of non-rigid airship (S. S. T. 14), the resistance coefficient of which had been found to be much smaller than any hitherto known (*see* R. & M. 607, Table 11, U.721). The dimensions of the model are given in Table 1, and a drawing in Fig. 1.

Information was required in some detail relating to the pressure distribution over the nose of the model; accordingly observations were taken (with a wind speed of 40 ft/sec.) at various angles of incidence and roll, *i.e.*, along the lines of intersection with the surface of several planes through the axis of the model, with the latter inclined at different angles to the direction of the wind.

At zero incidence the pressures were measured along the whole length of the model at wind speeds varying between 30 and 75 ft/sec., the pressure distribution at 40 ft./sec. having previously been examined in greater detail. For these observations the model was suspended on wires, thus avoiding the use of a spindle whose interference is always an uncertainty. All the experiments on the airship model were conducted in the 7-ft. channel, No. 2.

The usual method of measuring the pressures was adopted, viz., a length of soft composition tubing was sunk into the model, flush with the surface, irregularities being filled in with wax or plasticine. One end of the tube was stopped up airtight and the other end connected to one side of a tilting manometer. The other side of the gauge was connected to a hole in the side of the channel. The difference between the pressure at the position occupied by the model and the hole in the side of the channel has to be corrected for, and for this purpose the pressures along a line, coincident with the axis of the model, were measured (in the absence of the model) with the Static Pressure tube of the National Physical Laboratory standard pitot.

A small hole is made in the composition tubing at the point at which it is desired to measure the pressure; the hole is stopped up with plasticine after the observation has been taken and a new hole made, and so on.

Now as the tubing was only placed along one generator of the model, it was realised that to suspend the model on wires in a different attitude for each angle of yaw and roll would be a tedious process, whereas if a circular band were made and embedded in the model flush with the surface, and then attached

to a spindle placed in the chuck of the balance trumpet, it would be easy to change the angle of incidence by simply turning the balance through the desired angle, and the angle of roll could be altered by rotating the model about its axis, the circular band permitting this motion. Further, a detailed examination was only needed in the neighbourhood of the nose ; consequently it was thought that if the spindle were placed sufficiently far aft its presence would not be felt. A few observations were taken when the model was suspended on wires with the balance trumpet and spindle in place (20 inches aft of the nose of the model), and also with a dummy trumpet and spindle projecting successively from the roof and one side of the channel at the same distance from the nose. The pressure was measured at a point 15 inches from the nose, with the tube on the top of the model, and the presence of the trumpet could not be detected except when projecting from the roof. Accordingly, as it would not be necessary to rotate the model about its axis more than 90° from this position, and, further, no observations would be taken even as far as 15 inches from the nose of the model, it was considered quite safe to use a band and spindle in the manner described above.

In order to specify the different attitudes at which the pressures were observed, the system of axes recently adopted by the Aeronautical Society will be used. Taking the origin at the centre of volume of the model, the positive direction of the x axis is that opposite to the direction of the relative wind. The axis of z is vertically downwards, and that of y at right angles to both and to starboard. The angle of incidence α is zero when the axis of the model is along OX, and positive when it is turned from x to y. The angle of roll β is zero when the composition tubing in the model lies in the plane ZOX on the same side of OX as the positive direction of Z ; β is positive when the axial plane containing the tubing is rotated about OX in a direction y to z.

Observations were taken at angles of incidence varying between $-10°$ and $+10°$ by intervals of 2°, and at angles of roll varying between $-90°$ and $+90°$ by intervals of 20° or 30°. The wind speed was 40 ft/sec., and the pressures were measured as far as a point 5″ away from the nose, as it was believed that aft of that point the internal pressure in the envelope would always exceed the external pressure for all likely attitudes of the airship.

After consultation with Captain Rope, of Kingsnorth Airship Station, it was considered advisable to attempt to modify the form of the extreme nose and examine the effect on the pressures aft of the modified part. The modification adopted was as follows :—A small cone was made out of sheet tin and attached to the nose of the model, so that the circle of contact was approximately the section where the external pressure equalled the

internal pressure at zero incidence. The tangent cone touched the model $\frac{3}{4}$ inch from the original nose, the vertex being $\frac{7}{16}$ inch forward of the nose. The pressures were measured at points 0·85, 1, 1·5 and 2 inches from the nose, and as they were found to be very approximately equal to the pressures on the original model it was considered that the modification could, if necessary, be adopted without impairing the efficiency of the hull.

The results are given in the Tables and plotted as follows, the pressures being everywhere expressed as fractions of $\rho V^2/2$:—

	Table.	Fig.
Pressures along the model at zero incidence	2	—
Pressures along the model at wind speed 40 ft /sec.	—	1
Pressures on the nose at angles of yaw and roll—wind speed 40 ft /sec.	3	2
Effect of conical nose	4	1

As stated, the resistance of the model at zero incidence had been previously determined and hence it was considered advisable to integrate up the pressures given in Table 2, in order to ascertain what the magnitude of the so-called "form resistance" would be. Accordingly the integral $\frac{1}{V^2}\int p dA$ was calculated for different speeds, A being the area of the cross section of the model at right angles to its axis, and p the pressure at the section. The results obtained are worthy of note ; they show that the form resistance may be zero or even negative, or that the accuracy of the experiments is not sufficient to enable it to be found.

That this was not realised with previous pressure distribution experiments is due to the fact that this is the first time that the *variation* of static pressure along the axis of the channel has been taken into account. Hitherto a constant difference of pressure between the centre of the channel and the hole in the side of the channel had been assumed, viz., that at the balance, but in the present investigation, as has been noted, the difference between the pressures at the hole in the side and that at a point at any particular distance from the nose of the model (in the undisturbed channel) has been taken to correct the measured difference between the pressure at the hole in the side and that at a section the same distance from the nose of the model. Mention may be made of R. & M. 246 (v.), where it is stated that the "form resistance" is 14 per cent. of the total resistance of an airship model. Now if this be corrected for the spurious resistance due to pressure variation along the axis of the channel, it is reduced to 5 per cent. This spurious resistance and a method for determining it have been dealt with at length in R. & M. 564.

The method described there was sufficiently accurate to determine it when it was to be subtracted from the total resistance (of which it was about 15 to 20 per cent.), but that does not appear to be the case when only the form resistance is concerned, as the latter is of the same order of magnitude as the correction itself. In view of this, it seems highly desirable that experiments should be taken in hand immediately with a view to eliminating this correction altogether. It is proposed to use one of the smaller channels for the purpose, and to put in false sides so as to convert it into a diverging channel and so to eliminate the acceleration which corresponds with almost all the drop of pressure.

This uncertainty does not, however, reduce the value of the results as far as the original purpose of the experiments is concerned, as the pressures at the nose of the model are still sufficiently accurate for nose stiffening calculations to be based upon them.

A comparison of the drawing of the nose of the model with an ellipse, for which the ratio of the major to the minor axis $a/b = 4$, will show that the part of the model forward of the maximum cross section is very nearly an ellipsoid of revolution.

In view of this it was considered advisable to calculate theoretically the pressures in an ideal fluid over a spheroid for which $a/b = 4$ for different angle of incidence and roll. The values obtained are given in Table 5, and plotted in Figs. 3 and 4.

Mr. E. G. Gallop had already worked out the details of the problem analytically, and the authors wish to acknowledge their indebtedness to him for permission to use the following formulæ :—

If α be the angle the direction of the wind makes with the major axis, and if we consider the plane containing the major axis and the direction of the wind, the velocity potential over a spheroid is

$$-(\mathrm{A}\cos\alpha x + \mathrm{B}\sin\alpha y)\,\mathrm{V},$$

where V is the velocity of the wind,

$$\mathrm{A} = e^3 \div \left(e - \tfrac{1}{2}\frac{b}{a}\log\frac{1+e}{1-e}\right),$$

e being the eccentricity, and

$$\frac{1}{2\mathrm{A}} + \frac{1}{\mathrm{B}} = 1.$$

The maximum value of the velocity Q is given by

$$\mathrm{Q}^2 = (\mathrm{A}^2\cos^2\alpha + \mathrm{B}^2\sin^2\alpha)\,\mathrm{V}^2,$$

and $\mathrm{Q} > \mathrm{V}$, since $\mathrm{A} > 1$ and $\mathrm{B} > 1$.

If P_o be the point of zero velocity, η the angle the normal at P_o makes with the major axis, and ϕ_o the eccentric angle of P_o,

$$\tan \beta = \frac{B}{A} \tan \alpha, \tan \phi_o = \frac{b}{a} \frac{B}{A} \tan \alpha.$$

The pressure at P_o is $\frac{1}{2}\rho V^2 = 1$, say, then the pressure p, at a point P on the spheroid where the velocity is q is $1 - q^2/V^2$, and $q = Q \sin \varepsilon$, where ε is the angle between the normals at P_o and P. Therefore, if θ be the angle the normal at P makes with the major axis of the spheroid, $\varepsilon = \theta - \eta$ and

$$p = 1 - \frac{Q^2}{V^2} \sin^2 (\theta - \eta).$$

If ϕ be the eccentric angle of P, the relation connecting ϕ and θ is

$$\tan \phi = \frac{b}{a} \tan \theta.$$

If P does not lie in the vertical plane through the major axis, let the plane containing P and the major axis make an angle β with this vertical plane. In this case, ε still being the angle between the normals at P and P_o,

$$\cos \varepsilon = \cos \theta \cos \eta + \sin \theta \sin \eta \sin \beta,$$

and

$$p = 1 - \frac{Q^2}{V^2} \sin^2 \varepsilon = 1 - \frac{Q^2}{V^2} + \frac{Q^2}{V^2} (\cos \theta \cos \eta + \sin \theta \sin \eta \sin \beta)^2,$$

θ being given by $\tan \phi = \frac{b}{a} \tan \theta$ as before.

Before proceeding to a comparison between the pressures over the airship model and the theoretical pressures over the spheroid, it would be as well to compare the latter with the actual measured pressures over a spheroid. A model of a spheroid (semi axes 10 and 2·5 cms.) was made, and the distribution of pressure over it was measured in the No. 2 4-ft. channel at wind speeds of 40 and 60 ft/sec. The model was suspended by two wires, a small spike placed in the aft end of the model resting on a small streamline spindle placed in the balance chuck. Using the same axes as before to specify the attitude of the model, the pressures were examined (1) at zero incidence, (2) at angles of incidence of 10° and 20° for angles of roll $-90°$ and $+90°$, the observations at the two latter angles giving the maximum and minimum pressures for the particular angle of yaw under consideration. The observations have been corrected in the same manner as before for the drop of pressure in the channel, and the results expressed in terms of $\frac{1}{2}\rho V^2$ are given in Table 6, a mean of the values at 40 and 60 ft/sec. being given except in the neighbourhood of the tail, where a distinct speed effect was found and accordingly a few additional observations at 73 ft/sec. were taken. This irregularity may have been due

to the proximity of the spindle, but as theoretical and actual pressures at the extreme tail of a model can never be expected to agree it was not considered advisable to pursue the matter further, especially in view of the fact that the comparison was really needed only at the nose of the model. The results have been plotted against distance from the nose of the spheroid in Fig. 3. A glance at this figure shows that the agreement between theoretical and actual values is remarkably good, even for a good way along the model.

The general difference between the two sets of curves is that the pressure is greater (suction less) for the theoretical case than for the experimental. The deviation commences at about 1 cm. from the nose in the case of $\alpha = 0$, but the two curves come into closer agreement again at about 7 cms. For the windward side of the model the same remark applies, except that the curves do not begin to separate so close to the nose. It will be noticed that the agreement is much better on the windward side than it is on the leeward, the two curves on the latter side being appreciably different.

The calculated theoretical pressures on the spheroid are plotted in Fig. 4 against angle of roll for various angles of yaw at different distances from the nose, the latter being expressed in terms of the eccentric angle ϕ, *i.e.*, the distance from the nose is $a(1 - \cos \phi)$ where $2a$ = the overall length of the model. A comparison with Fig. 2 shows how similar the curves for the experimental pressures on the airship are to those for the theoretical pressures on the spheroid. The pressures on the spheroid at $\alpha = 20°$ have been added in order to show how the pressure distribution on the nose of the airship model may vary with angle of roll at an angle of yaw of 20°.

A comparison between theoretical and actual pressures over a series of models similar to airship models is given at zero incidence by Fuhrmann in *Jahrbuch d. Motorluftschiff Studiengesellschaft*, 1911–12. The agreement there is also very good. There is one model with a spheroidal head, but as there are no means of ascertaining whether or not the experimental results given there have been corrected for static pressure variation, even though mention is made of several other corrections, it did not appear necessary to compare with the present results.

Returning again to a comparison of the nose of the airship model with a spheroid, it will be seen from Fig. 5 that the extreme nose of the generator of the airship model is not so bluff as that of the ellipse ; the airship generator lies inside the ellipse for a short distance, then it crosses and remains outside as far as the maximum ordinate. The same figure shows that the theoretical pressures on the spheroid at zero incidence are less than those on the airship model near the nose.

Now, in view of the fact that adding the tangent cone to the nose of the airship model did not appear to affect the pressures aft of the circle of contact for $\alpha = \theta$, the only difference being that brought about by moving the $\rho V^2/2$ point further forward (*see* Fig. 1), it was thought that if a spheroid were found to fit the airship model a short distance aft of the nose, and the theoretical pressures on that spheroid calculated, *placing the* $\rho V^2/2$ *point at the nose of the airship model*, the pressure curves might be brought into closer agreement. Accordingly this was done ; two spheroids were found and the pressures calculated. The results are given in Table 7 and plotted in Fig. 6. It is immediately evident that the pressure curves agree remarkably well for either spheroid forward of the point where the pressure is 1/10 of ρV^2, and this is the region that is most important for nose-stiffening purposes.

It would thus appear that nose-stiffening calculations on any airship model, with a head of approximately spheroidal form, could be based on calculated pressures over a spheroid which fits the head of the airship near the nose, always bearing in mind that the point of maximum pressure at zero angle of incidence is at the nose of the airship (not the nose of the spheroid) and that the pressure there is $\rho V^2/2$ as usual.

TABLE 1.

DIMENSIONS OF MODEL U.721.

Distance from nose. / Maximum diameter.	Diameter. / Maximum diameter.	Distance from nose. / Maximum diameter.	Diameter. / Maximum diameter.
0	0	2·096	0·999
0·058	0·219	2·328	0·986
0·116	0·331	2·611	0·957
0·175	0·418	2·794	0·913
0·233	0·482	3·027	0·852
0·291	0·524	3·260	0·776
0·349	0·586	3·376	0·733
0·407	0·629	3·492	0·689
0·466	0·665	3·609	0·638
0·582	0·730	3·725	0·584
0·698	0·785	3·842	0·525
0·931	0·866	3·958	0·462
1·164	0·924	4·074	0·396
1·397	0·963	4·191	0·324
1·630	0·984	4·307	0·247
1·863	0·998	4·424	0·166
1·979	1·000	4·540	0·077
		4·622	0

Overall length, 39·7″.
Maximum diameter, 8·59″.

TABLE 2.

VARIATION OF PRESSURE DISTRIBUTION ALONG THE SURFACE OF THE MODEL AT ZERO ANGLE OF INCIDENCE.

Distance from nose.	Wind speed, ft./sec.							Mean of all results.
	30	40	50	60	70	75	Previous result 40.	
0·25	—	—	—	—	—	—	0·760	—
0·5	0·550	0·547	0·547	0·547	0·541	0·541	0·550	0·546
0·75	—	—	—	—	—	—	0·300	—
1	0·241	0·232	0·232	0·228	0·225	0·224	0·206	0·227
1·5	—	—	—	—	—	—	0·085	—
2	0·018	0·017	0·018	0·017	0·019	0·020	0·006	0·015
3	−0·070	−0·074	−0·077	−0·077	−0·081	−0·081	−0·087	−0·078
4	−0·107	−0·106	−0·105	−0·105	−0·106	−0·107	−0·110	−0·107
4·5	—	—	—	—	—	—	−0·133	—
5	−0·140	−0·138	−0·136	−0·136	−0·136	−0·135	−0·141	−0·138
6	−0·150	−0·151	−0·149	−0·151	−0·151	−0·151	−0·156	−0·151
7	−0·177	−0·175	−0·179	−0·180	−0·183	−0·185	−0·173	−0·179
8	−0·179	−0·179	−0·182	−0·182	−0·183	−0·186	−0·181	−0·182
9	−0·178	−0·176	−0·176	−0·175	−0·176	−0·178	−0·187	−0·178
11	−0·181	−0·181	−0·181	−0·182	−0·183	−0·184	−0·178	−0·182
13	−0·166	−0·168	−0·169	−0·171	−0·173	−0·168	−0·166	−0·169
15	−0·160	−0·157	−0·158	−0·158	−0·159	−0·159	−0·160	−0·159
17	—	—	—	—	—	—	−0·177	—
19	−0·180	−0·180	−0·181	−0·178	−0·178	−0·177	−0·192	−0·181
21	—	—	—	—	—	—	−0·175	—
23	−0·160	−0·162	−0·164	−0·164	−0·166	−0·166	−0·154	−0·162
25	—	—	—	—	—	—	−0·126	—
27	−0·098	−0·103	−0·109	−0·108	−0·100	−0·098	−0·099	−0·102
29	—	—	—	—	—	—	−0·059	—
31	−0·042	−0·020	−0·016	−0·021	−0·023	−0·025	−0·020	−0·019
33	—	—	—	—	—	—	0·038	—
35	—	—	—	—	—	—	0·101	—
36	—	—	—	—	—	—	0·139	—
37	—	—	—	—	—	—	0·173	—
38	—	—	—	—	—	—	0·196	—

TABLE 3.

VALUES OF PRESSURE/$\frac{1}{2}\rho V^2$ OVER AIRSHIP MODEL U.721 AT DIFFERENT ANGLES OF YAW AND ROLL.

Wind speed, 40 ft/sec.

Distance from nose, 0.

Angle of Yaw.	Pressure / $\frac{1}{2}\rho V^2$
0°	1·000
2°	0·997
4°	0·976
6°	0·954
8°	0·911
10°	0·866

TABLE 3.—*continued.*

Distance from nose, 0″·15.

Angle of Yaw.	Angle of Roll.		
	−90°	0°	90°
0°	0·935	0·931	0·935
2°	0·905	0·931	0·964
4°	0·865	0·915	0·976
6°	0·816	0·898	0·988
8°	0·764	0·877	0·992
10°	0·698	0·836	0·990

Distance from nose, 0″·25.

Angle of Yaw.	Angle of Roll.								
	−90°	−70°	−50°	−30°	0°	30°	50°	70°	90°
0°	0·715	0·712	0·710	0·710	0·719	0·710	0·710	0·712	0·715
2°	0·651	0·653	0·662	0·675	0·708	0·729	0·751	0·763	0·765
4°	0·582	0·584	0·607	0·636	0·691	0·754	0·788	0·815	0·823
6°	0·508	0·516	0·536	0·579	0·670	0·761	0·816	0·852	0·866
8°	0·428	0·441	0·470	0·519	0·637	0·763	0·834	0·889	0·905
10°	0·352	0·363	0·392	0·460	0·600	0·760	0·853	0·917	0·934

Distance from nose, 0″·5.

Angle of Yaw.	Angle of Roll.								
	−90°	−70°	−50°	−30°	0°	30°	50°	70°	90°
0°	0·530	0·533	0·533	0·533	0·531	0·533	0·533	0·533	0·534
2°	0·460	0·466	0·478	0·493	0·527	0·560	0·576	0·592	0·600
4°	0·386	0·394	0·417	0·449	0·514	0·584	0·624	0·652	0·666
6°	0·312	0·320	0·350	0·400	0·492	0·599	0·660	0·706	0·723
8°	0·234	0·244	0·280	0·341	0·463	0·611	0·691	0·752	0·776
10°	0·156	0·165	0·207	0·272	0·428	0·611	0·713	0·795	0·818

Distance from nose, 1″.

Angle of Yaw.	Angle of Roll.								
	−90°	−70°	−50°	−30°	0°	30°	50°	70°	90°
0°	0·234	0·236	0·234	0·236	0·230	0·236	0·234	0·236	0·234
2°	0·162	0·167	0·177	0·199	0·232	0·266	0·280	0·297	0·302
4°	0·091	0·101	0·120	0·154	0·220	0·296	0·333	0·369	0·375
6°	+0·017	+0·032	+0·059	0·110	0·205	0·314	0·376	0·424	0·437
8°	−0·055	−0·036	−0·007	+0·053	0·180	0·333	0·416	0·476	0·503
10°	−0·127	−0·112	−0·072	−0·004	0·150	0·340	0·447	0·532	0·561

TABLE 3—*continued.*

Distance from nose, 1″·4.

Angle of Yaw.	Angle of Roll.								
	−90°	−70°	−50°	−30°	0°	30°	50°	70°	90°
0°	0·105	0·101	0·103	0·107	0·107	0·107	0·103	0·101	0·105
2°	+0·038	+0·040	0·055	0·070	0·103	0·133	0·152	0·162	0·169
4°	−0·026	−0·021	+0·002	+0·032	0·093	0·162	0·194	0·222	0·236
6°	−0·087	−0·085	−0·055	−0·009	0·078	0·181	0·228	0·278	0·300
8°	−0·158	−0·143	−0·110	−0·061	0·055	0·196	0·282	0·336	0·361
10°	−0·217	−0·201	−0·171	−0·114	0·026	0·203	0·310	0·396	0·418

Distance from nose, 2″.

Angle of Yaw.	Angle of Roll.								
	−90°	−70°	−50°	−30°	0°	30°	50°	70°	90°
0°	−0·011	−0·008	−0·008	−0·008	−0·006	−0·008	−0·008	−0·008	−0·011
2°	−0·074	−0·068	−0·053	−0·042	−0·013	+0·017	+0·038	+0·047	+0·051
4°	−0·135	−0·127	−0·103	−0·082	−0·021	0·040	0·084	0·105	0·106
6°	−0·194	−0·184	−0·154	−0·124	−0·038	0·059	0·124	0·163	0·175
8°	−0·251	−0·242	−0·215	−0·169	−0·063	0·076	0·163	0·219	0·238
10°	−0·308	−0·299	−0·272	−0·222	−0·091	0·082	0·200	0·274	0·300

Distance from nose, 3″.

Angle of Yaw.	Angle of Roll.						
	−90°	−60°	−30°	0°	30°	60°	90°
0°	−0·055	−0·057	−0·057	−0·055	−0·057	−0·057	−0·055
2°	−0·105	−0·099	−0·086	−0·057	−0·036	−0·015	−0·008
4°	−0·152	−0·143	−0·114	−0·065	−0·015	+0·025	+0·042
6°	−0·200	−0·184	−0·150	−0·082	−0·002	0·065	0·099
8°	−0·240	−0·232	−0·188	−0·103	+0·006	0·106	0·154
10°	−0·282	−0·274	−0·232	−0·133	0·008	0·142	0·203

Distance from nose, 4″.

Angle of Yaw.	Angle of Roll.						
	−90°	−60°	−30°	0°	30°	60°	90°
0°	−0·116	−0·114	−0·112	−0·112	−0·112	−0·114	−0·116
2°	−0·156	−0·150	−0·135	−0·114	−0·097	−0·080	−0·072
4°	−0·196	−0·184	−0·165	−0·125	−0·087	−0·042	−0·028
6°	−0·230	−0·222	−0·194	−0·144	−0·074	−0·009	+0·019
8°	−0·262	−0·258	−0·234	−0·165	−0·068	+0·025	0·065
10°	−0·292	−0·291	−0·274	−0·196	−0·068	0·059	0·125

TABLE 3—*continued.*

Distance from nose, 5″.

Angle of Yaw.	Angle of Roll.						
	−90°	−60°	−30°	0°	30°	60°	90°
0°	−0·141	−0·141	−0·139	−0·139	−0·139	−0·141	−0·141
2°	−0·175	−0·171	−0·158	−0·142	−0·123	−0·114	−0·106
4°	−0·206	−0·206	−0·179	−0·152	−0·110	−0·087	−0·065
6°	−0·236	−0·238	−0·207	−0·167	−0·105	−0·055	−0·023
8°	−0·279	−0·264	−0·238	−0·188	−0·103	−0·026	+0·017
10°	−0·285	−0·291	−0·272	−0·213	−0·103	−0·004	0·061

TABLE 4.

VALUES OF PRESSURE/$\frac{1}{2}\rho V^2$ ON THE MODEL WITH THE CONICAL NOSE ATTACHED.

Distance from nose, 0″·85.

Angle of Yaw.	Angle of Roll.		
	−90°	0°	90°
0°	+0·324	0·320	0·324
10°	−0·021	0·221	0·632

Distance from nose, 1″.

Angle of Yaw.	Angle of Roll.		
	−90°	0°	90°
0°	+0·247	0·246	0·247
10°	−0·010	0·148	0·564

Distance from nose, 1″·5.

Angle of Yaw.	Angle of Roll.		
	−90°	0°	90°
0°	+0·087	0·087	0·087
10°	−0·228	0·008	0·402

TABLE 4—*continued.*

Distance from nose, 2″.

Angle of Yaw.	Angle of Roll.		
	−90°	0°	90°
0°	+0·002	−0·002	0·002
10°	−0·0288	−0·086	0·312

Circle of contact of conical nose $\frac{3}{4}''$ from nose of model.
Vertex of cone $\frac{7}{16}''$ from nose of model.

TABLE 5.

THEORETICAL CASE—PRESSURE DISTRIBUTION OVER A PROLATE SPHEROID, $a/b = 4$.

Angle of yaw, $\alpha = 0$.			$\alpha = 20°$.		
Distance from nose ÷ Maximum diameter.	ϕ	Pressure $\frac{1}{2}\rho V^2$	ϕ	Pressure $\frac{1}{2}\rho V^2$	
				Angle of Roll.	
				$\beta = 90°$	$\beta = -90°$
0	0°	1	0°	0·595	0·595
0·010	5°	0·87	5°	0·929	+0·120
0·023	10°	0·61	10°	0·996	−0·224
0·069	15°	0·37	15°	0·903	−0·389
0·123	20°	0·20	20°	0·771	−0·439
0·269	30°	+0·03	25°	0·660	−0·439
0·469	40°	−0·07	30°	0·537	−0·408
0·665	50°	−0·12	40°	0·372	−0·339
1·315	70°	−0·16	50°	0·253	−0·265
2·00	90°	−0·17	70°	+0·088	−0·146
—	—	—	90°	−0·033	−0·033

TABLE 5—*continued.*

$\alpha = 4°$.

ϕ	Pressure / $\frac{1}{2}\rho V^2$						
	$\beta = 90°$	60°	30°	0°	−30°	−60°	−90°
0°	0·982	0·982	0·982	0·982	0·982	0·982	0·982
5°	0·949	0·938	0·901	0·859	0·817	0·781	0·772
10°	0·729	0·710	0·659	0·594	0·532	0·479	0·469
15°	0·507	0·487	0·430	0·359	0·291	0·245	0·229
20°	0·331	0·313	0·259	0·191	+0·129	+0·087	+0·073
30°	0·118	+0·100	+0·056	+0·002	−0·045	−0·075	−0·085
40°	+0·006	−0·007	−0·043	−0·086	−0·120	−0·140	−0·147
50°	−0·059	−0·071	−0·100	−0·132	−0·156	−0·168	−0·172
70°	−0·129	−0·137	−0·155	−0·171	−0·180	−0·181	−0·180
90°	−0·164	−0·168	−0·177	−0·181	−0·177	−0·168	−0·164

$\alpha = 6°$.

ϕ	Pressure / $\frac{1}{2}\rho V^2$						
	$\beta = 90°$	60°	30°	0°	−30°	−60°	−90°
0°	0·953	0·953	0·953	0·953	0·953	0·953	0·953
5°	0·953	0·943	0·903	0·833	0·772	0·727	0·712
10°	0·787	0·755	0·666	0·573	0·480	0·413	0·390
15°	0·567	0·534	0·448	0·340	0·240	0·173	0·151
20°	0·393	0·360	0·275	+0·172	+0·081	+0·022	+0·003
30°	0·169	0·142	+0·069	−0·015	−0·083	−0·123	−0·135
40°	+0·046	+0·022	−0·037	−0·103	−0·156	−0·176	−0·182
50°	−0·028	−0·048	−0·097	−0·148	−0·181	−0·194	−0·197
70°	−0·113	−0·127	−0·167	−0·187	−0·197	−0·189	−0·188
90°	−0·158	−0·169	−0·187	−0·197	−0·187	−0·169	−0·158

$\alpha = 10°$.

ϕ	Pressure / $\frac{1}{2}\rho V^2$						
	$\beta = 90°$	60°	30°	0°	−30°	−60°	−90°
0°	0·900	0·900	0·900	0·900	0·900	0·900	0·900
5°	0·998	0·965	0·880	0·775	0·670	0·600	0·573
10°	0·876	0·820	0·686	0·516	0·361	0·261	+0·230
15°	0·686	0·627	0·470	0·285	+0·129	+0·030	0
20°	0·515	0·451	0·301	+0·122	−0·020	−0·106	−0·120
30°	0·279	0·220	+0·085	−0·062	−0·165	−0·212	−0·220
40°	0·140	0·088	−0·029	−0·147	−0·217	−0·238	−0·240
50°	+0·048	+0·012	−0·098	−0·192	−0·237	−0·237	−0·230
70°	−0·065	−0·102	−0·175	−0·231	−0·236	−0·207	−0·190
90°	−0·140	−0·162	−0·214	−0·240	−0·214	−0·162	−0·140

ϕ = Eccentric angle.

If $2a$ = overall length of model and $2b$ the maximum diameter, then distance from nose $= a\ (1 - \cos \phi)$, distance from nose ÷ maximum diameter $= \frac{a}{2b}(1 - \cos \phi)$

$= 2\ (1 - \cos \phi)$ when $a/b = 4$.

TABLE 6.

PRESSURE DISTRIBUTION OVER ELLIPSOID.

Axes, 20 cms. and 5 cms.

Pressure / $\frac{1}{2}\rho V^2$.

Distance from nose ÷ Max. diam.	Eccentric angle, ϕ.	Angle of Incidence, 0°.	Angle of Incidence, 10°.		Angle of Incidence, 20°.	
			Tube to Windward.	Tube to Leeward.	Tube to Windward.	Tube to Leeward.
0	0°	0·960	0·898	0·876	0·588	0·561
0·010	5°	0·825	0·985	0·526	0·924	+0·134
0·023	10°	0·591	0·880	0·229	0·963	−0·220
0·069	15°	0·406	0·719	+0·038	0·904	−0·395
0·123	20°	0·168	0·494	−0·192	0·768	−0·503
0·188	25°	+0·044	0·342	−0·254	0·609	−0·494
0·269	30°	−0·013	0·220	−0·266	0·520	−0·451
0·363	35°	−0·061	0·161	−0·242	0·431	−0·374
0·469	40°	−0·088	0·110	−0·254	0·342	−0·352
0·537	45°	−0·113	0·068	−0·225	0·281	−0·323
0·854	55°	−0·125	+0·003	−0·225	0·208	−0·251
1·155	65°	−0·154	−0·059	−0·215	0·117	−0·204
1·483	75°	−0·168	−0·112	−0·196	0·044	−0·154
1·739	82·5°	−0·171	−0·121	−0·175	+0·004	−0·127
2·000	90°	−0·183	−0·150	−0·161	−0·060	−0·096
2·261	97·5°	−0·176	−0·175	−0·140	−0·082	−0·062
2·517	105°	−0·160	−0·167	−0·103	−0·115	−0·030
2·845	115°	−0·142	−0·198	−0·073	−0·152	−0·012
3·146	125°	−0·120	−0·196(*a*) −0·216(*b*)	−0·036	−0·190(*a*) −0·202(*b*) −0·214(*c*)	−0·008(*a*) +0·002(*b*)
3·463	135°	−0·093	−0·153(*a*) −0·182(*b*)	−0·004(*a*) +0·015(*b*) +0·019(*c*)	−0·190(*a*) −0·208(*b*) −0·220(*c*)	−0·019(*a*) +0·015(*b*) +0·017(*c*)
3·637	145°	−0·063(*a*) −0·041(*b*)	−0·078(*a*) −0·128(*b*) −0·143(*c*)	−0·030(*a*) +0·048(*b*) +0·054(*c*)	−0·140(*a*) −0·194(*b*) −0·223(*c*)	−0·070(*a*) −0·008(*b*) +0·060(*c*)
3·731	150°	−0·013(*a*) −0·036(*b*)	−0·067(*a*) −0·092(*b*) −0·094(*c*)			
3·812	155°	+0·060(*a*) +0·106(*b*)	−0·033(*a*) −0·016(*b*) +0·001(*c*)			
3·877	160°	0·103(*a*) 0·155(*b*) 0·160(*c*)				
3·931	165°	0·131(*a*) 0·175(*b*) 0·184(*c*)				

(*a*) Wind speed = 40 ft/sec.
(*b*) Wind speed = 60 ft/sec.
(*c*) Wind speed = 72·8 ft/sec.

The remaining observations are means of the values at 40 and 60 ft/sec.

Wind Speed - 40 f/s

Pressure expressed in terms of $\frac{1}{2}\rho V^2$.

Shaded part at nose shows tangent cone added pressures with tangent cone attached.

Scale of drawing of model $\frac{1}{4.36}$ model size.

Overall length	39.7"
Max: diameter	8.59"

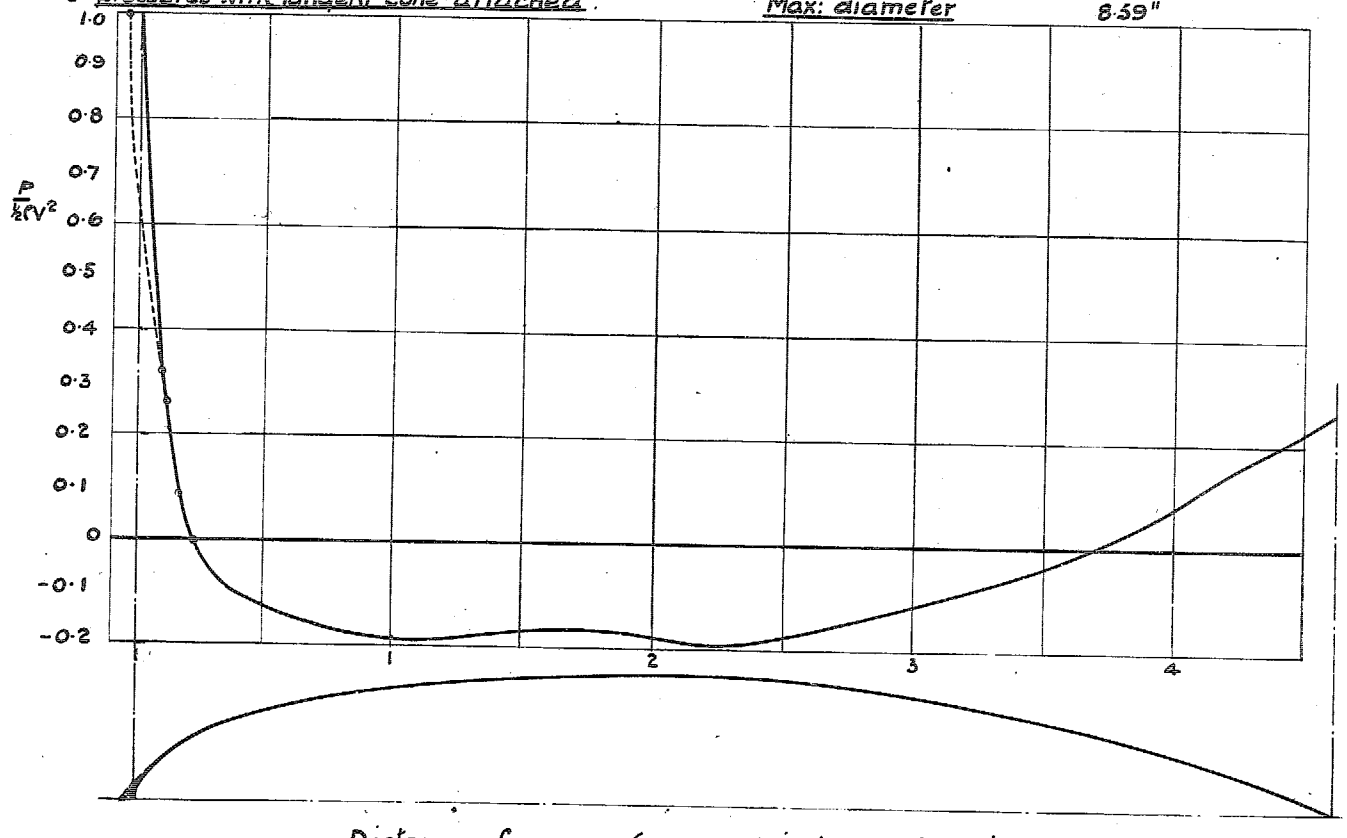

FIG. 1.

PRESSURE DISTRIBUTION OVER THE NOSE OF AN AIRSHIP MODEL.

Variations of Pressure with Angles of Yaw and Roll. Pressures expressed in terms of $\frac{1}{2}\rho V^2$.

FIG 2.

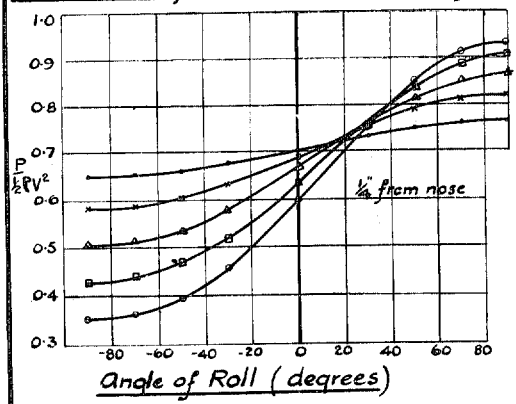

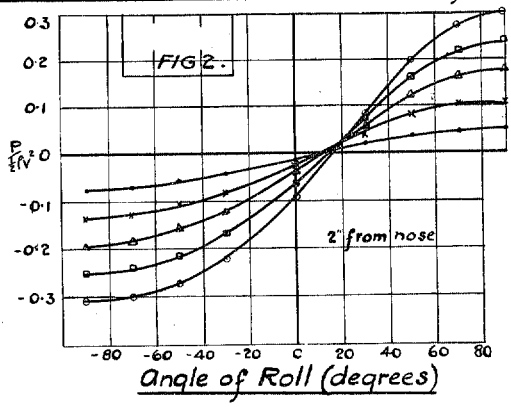

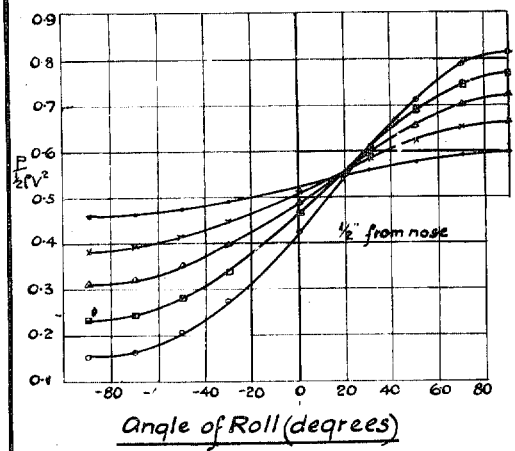

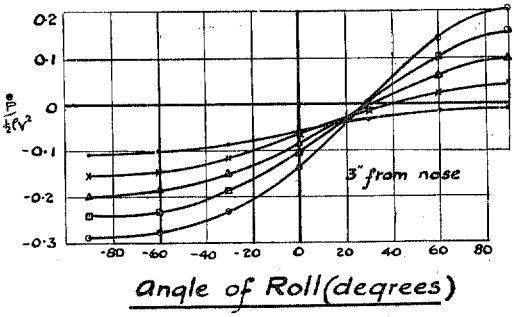

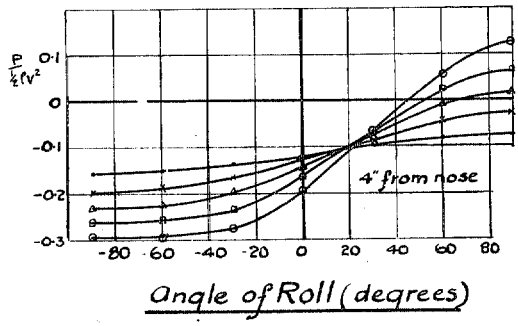

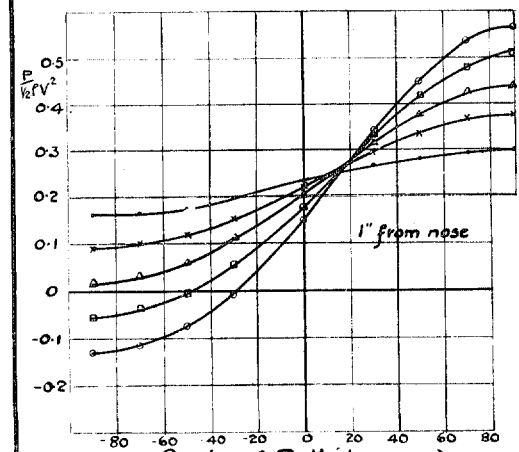

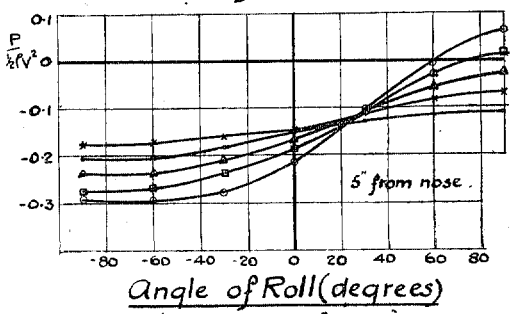

· Angle of Yaw 2°
× " " " 4°
△ " " " 6°

⊡ Angle of Yaw 8°
⊙ " " " 10°

PRESSURE DISTRIBUTION over a SPHEROID

—— Theoretical Pressure

---- Actual Measured "

FIG.3.

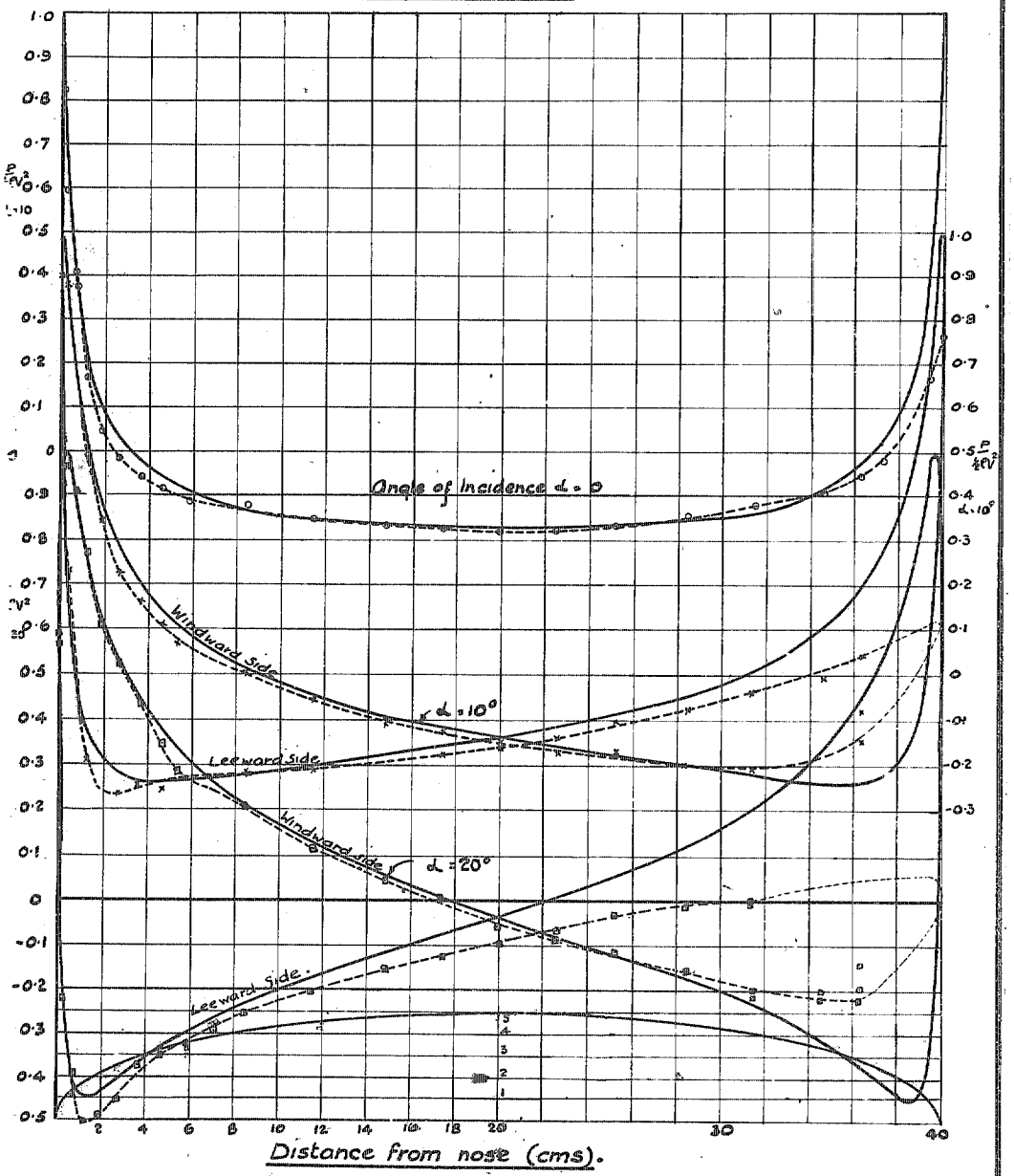

PRESSURE DISTRIBUTION OVER A SPHEROID.

Variation of pressure with angles of yaw and roll. Pressures expressed in terms of $\frac{1}{2}\rho V^2$.

Fig.4.

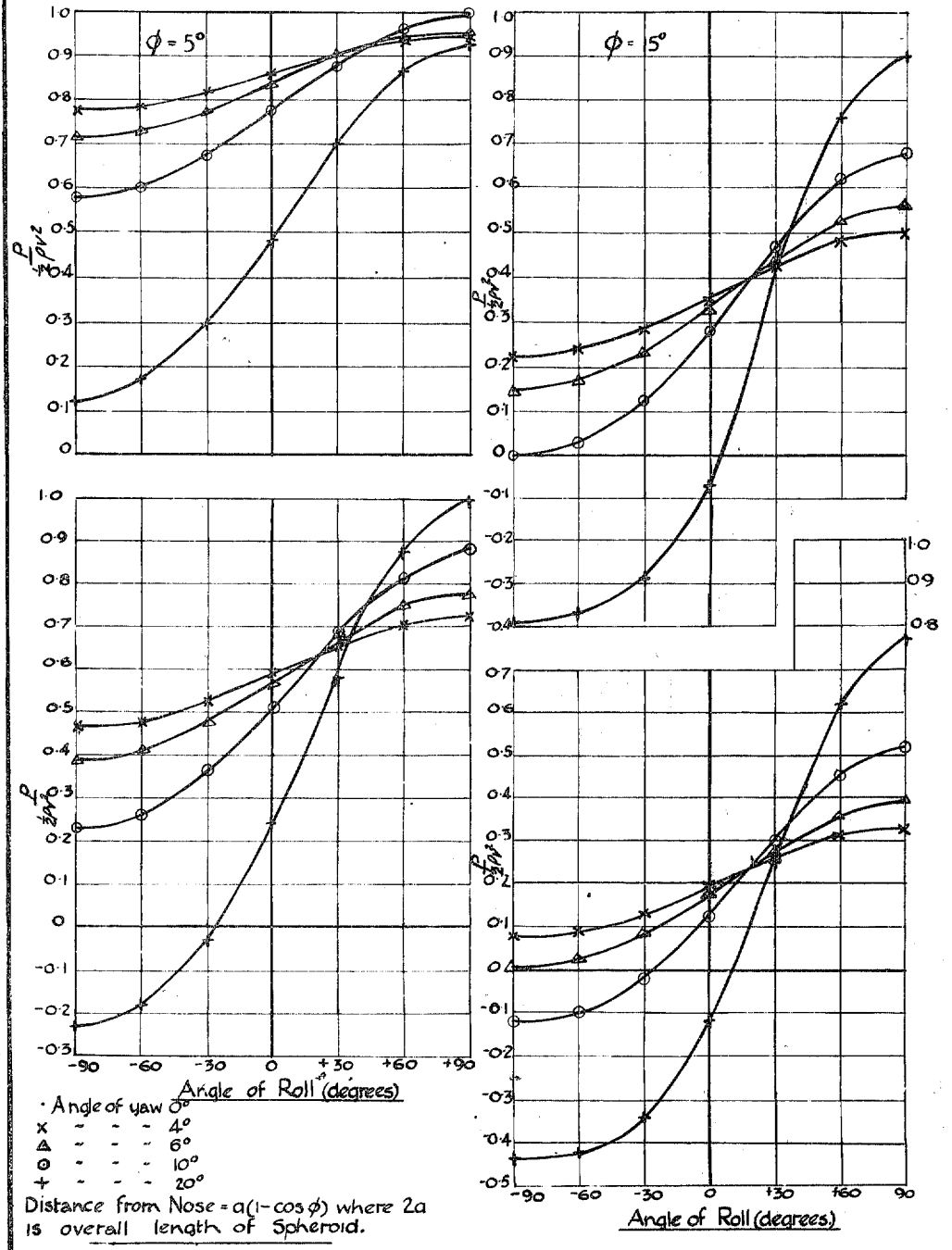

· Angle of yaw 0°
× ~ ~ ~ 4°
△ ~ ~ ~ 6°
⊙ ~ ~ ~ 10°
\+ ~ ~ ~ 20°

Distance from Nose = a(1 − cos φ) where 2a is overall length of Spheroid.

FIG. 5.

PRESSURE DISTRIBUTION OVER THE NOSE OF AIRSHIP MODEL U.721.

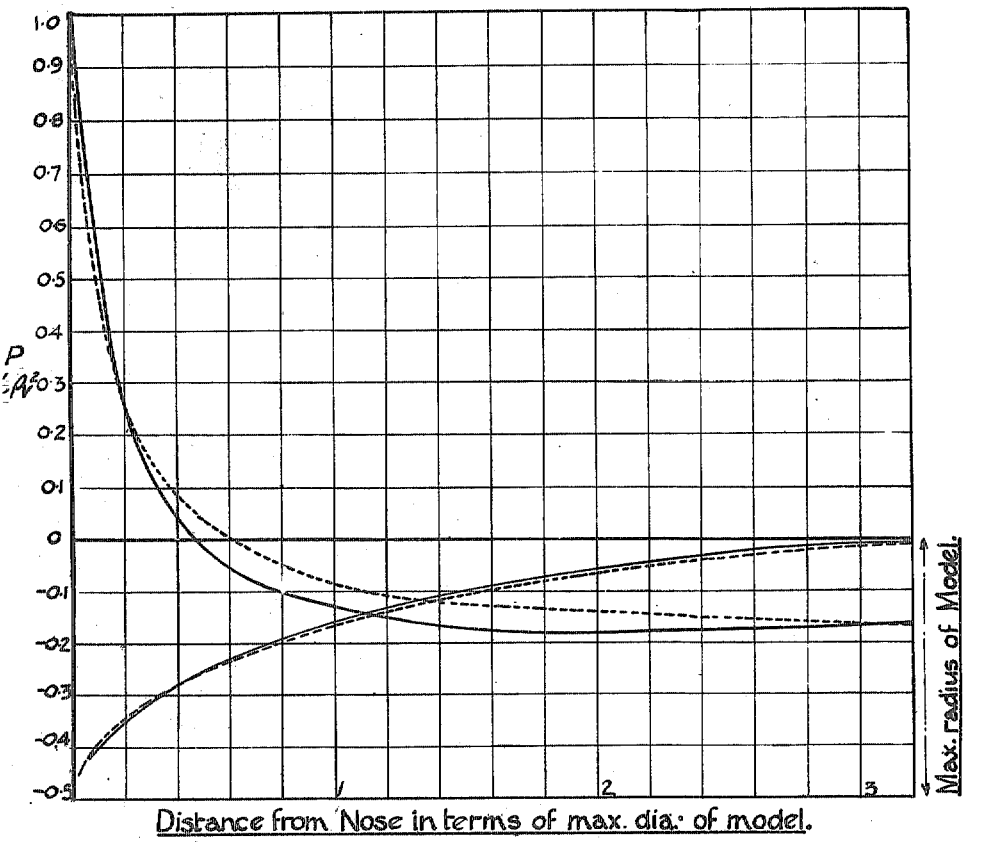

Distance from Nose in terms of max. dia. of model.

——— Airship Model and pressures on it in terms of $\frac{\rho V^2}{2}$.

--------Spheroid Ratio of axes 4:1 in terms of $\frac{\rho V^2}{2}$.

FIG. 6.

PRESSURE DISTRIBUTION OVER THE NOSE OF AIRSHIP MODEL U. 721.

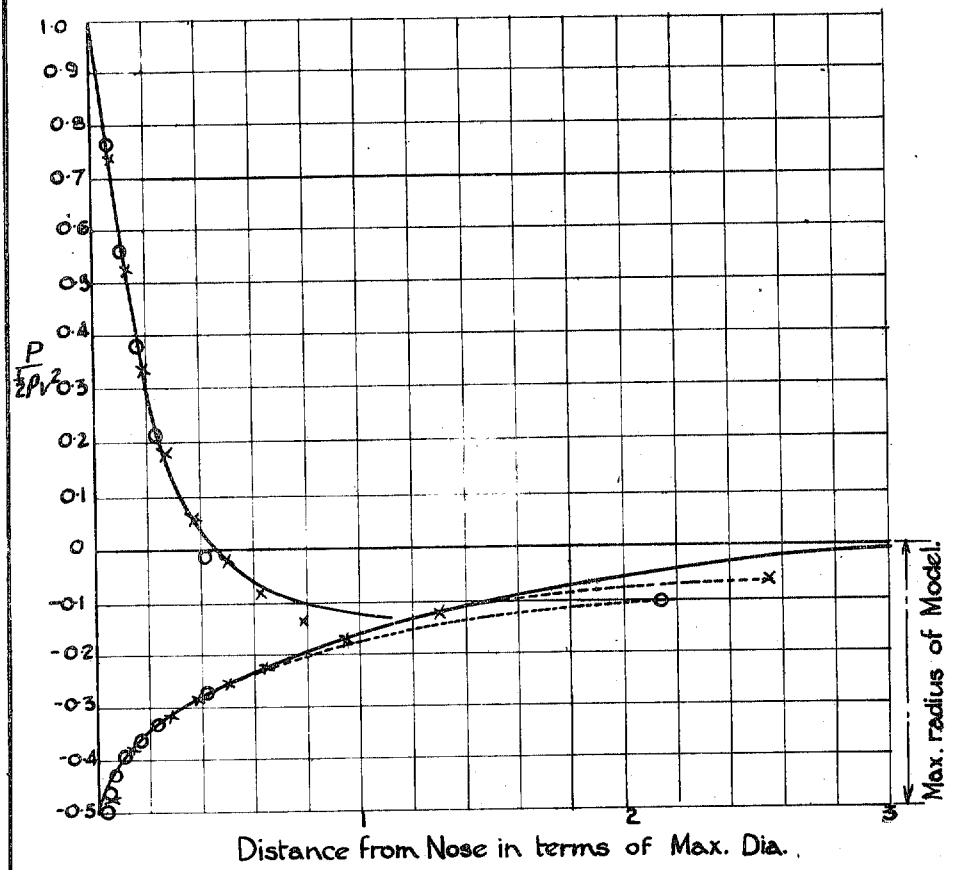

Full curve = Airship Model and pressures on it in terms of $\frac{\rho V^2}{2}$.

⊙ = Spheroid ratio of axes 2·65 & pressures on it in terms of $\frac{\rho V^2}{2}$.

× = Spheroid ratio of axes 2·89 & pressures on it in terms of $\frac{\rho V^2}{2}$.

TABLE 7.

COMPARISON OF PRESSURES OVER THE NOSE OF THE MODEL WITH THOSE OVER SPHEROIDS APPROXIMATING TO THE NOSE.

Take the minor axis of the model to be 10. The equation to the ellipse will be $\frac{(x-\xi)^2}{a^2}+\frac{y^2}{b^2}=1$ if the origin of co-ordinates be at the nose of the airship model, ξ the distance of the centre of the ellipse from the origin.

(1) Ellipse through the points (0·5821, 1·0943), (1·7462, 2·0896), (2·3283, 2·4097).

$\xi = 10{\cdot}74.$ $a = 10{\cdot}55.$ $b = 3{\cdot}98.$ $a/b = 2{\cdot}65.$

ϕ	$\frac{\text{Pressure}}{\frac{1}{2}\rho V^2}$	$\frac{x}{\text{Maximum diam. of airship model}}$
0°	1	0·19
5°	0·933	0·23
10°	0·765	0·35
15°	0·560	0·54
20°	0·370	0·83
25°	+0·209	1·18
35°	−0·015	2·10

(2) Ellipse through the points (1·7462, 2·0896), (4·0745, 3·1432), (5·8207, 3·6496).

$\xi = 12{\cdot}79.$ $a = 12{\cdot}58.$ $b = 4{\cdot}36.$ $a/b = 2{\cdot}885.$

ϕ	$\frac{\text{Pressure}}{\frac{1}{2}\rho V^2}$	$\frac{x}{\text{Maximum diam. of airship model}}$
0°	1	0·21
5°	0·924	0·28
10°	0·738	0·40
15°	0·524	0·65
20°	0·334	0·99
25°	0·180	1·39
30°	+0·063	1·90
35°	−0·020	2·50